PARAMETER IDENTIFICATION USING ROLSM IN PROBLEMS OF FIRE TECHNOLOGY

Jukka Myllymäki & Djebar Baroudi

Rakenteiden Mekaniikka, Vol. 29
Nro 3-4, 1996, s. 87-102

ABSTRACT

This work presents a global, reliable and systematic methodology, regularized output least square method (ROLSM), to treat parameter identification problems. Several applications of the method to parameter identification in the problems of fire technology are presented. Numerical examples of heat transfer in insulated and bare metal structures are presented. For each problem one ordinary differential equation is derived from the variational formulation of the general heat conduction problem. As an example of the use of the method to mechanical properties of metals an identification of multiplicative viscoplasticity law for aluminium alloy AA6063-T6 is illustrated. Since the inverse problem is usually ill-posed regularization is needed. Both regularization using mesh coarsing and Tikhonov-regularization (penalized output least square method) are used in order to get stabilized solution. The unknown distributed parameters are discretized using continuous piecewise linear basis functions.

NOMENCLATURE

c, c_p, c_s	specific heat, specific heat of fire protection, specific heat of metal structure J/(kg K)
d, d_p, d_s	thickness, thickness of fire protection, thickness of metal structure, m
$\mathbf{f}$	force vectors
q	heat flux, W/m^2
t	time, s
x	space dimension, m
A_p, A_s	area of the fire protection and metal structure, m^2
$\mathbf{C}$	capacitance matrix
$\mathbf{K}$	conductance matrix
N_i	shape functions
$Q_s = \rho_s A_s c_s d_s$	thermal capacity of the metal structure, J/ K
$Q_p = \rho_p A_p c_p d_p$	thermal capacity of the fire protection, J/ K
Q_{ij}^p	elements of capacity matrix of the fire protection, J/ K
T, T_p,	temperature, temperature of protection, K
T_s, T_g	temperature of metal structure and surrounding gas, K
$\mathbf{T}$	degrees of freedom, temperature vector, K
ε, ε_r, ε_g	emissivity, resultant emissivity and emissivity of the gas

λ, λ_p, λ_s	thermal conductivity, thermal conductivity of protection and of metal structure, W/m K
v	test function
ρ, ρ_p, ρ_s	density, density of fire protection and of metal structure kg/m^3
ξ_K	co-ordinates of the Gauss-integration points

INTRODUCTION

An *inverse problem* is a problem which is posed as inverted compared to *direct* problems. The type of a direct problem [1] considered here is in determining the effect y caused by x when a definite mathematical model K is stated: $Kx = y$. For such direct problems we assume that the operator K is well-defined and continuous. Therefore there exists a unique effect of y for each cause x; and small changes in x result in small changes in y. Given a direct problem of the type just discussed, two inverse problems may be immediately posed. These are the inverse problems of causation (given K and y, determine x) and model identification (given x and y, determine K). In the direct problems the existence, uniqueness and stability of solutions is assumed, but in inverse problems none of these properties can be taken as granted [1].

A common feature of inverse problems is the *instability,* that is, small changes in the data may give rise to large changes in the solution. The computational treatment of such problems requires discretization. Small finite dimensional problems are typically stable, however, as the discretization is refined, the number of variables increases and the instability of the original problem becomes apparent in the discrete model [1].

The applications illustrated in this paper, the model identification problems in the field of fire technology, are of the latter type of the two discussed above. The problems treated are heat transfer as a one variable problem in uninsulated and insulated metal structures and one dimensional form of viscoplastic constitutive equation for metals at high temperatures.

FORMULATION OF THE PROBLEM

Consider a coefficient determination problem, i.e. the problem of determining a non-constant coefficient a in an initial value problem (Cauchy problem)

$$\dot{y} = a(y)y + f(y), \quad y(0) = y_o \tag{1}$$

on the base of the existing data about the solution y.

We may interpret this in terms of a coefficient-to-solution operator

$$F(a) = y \tag{2}$$

where the operator F is defined by

$$F(a(y), y, t) = y(0) + \int_0^t \{a(y)y + f(y)\}\, d\tau \tag{3}$$

Equation (3) has to be discretized in to chosen number of sub-intervals $[t_k, t_{k+1}]$;

$$y^n = y^{n-1} + \int_{t_{n-1}}^{t_n} \{a(y)y + f(y)\}\, d\tau \qquad (4)$$

Depending on the integration scheme used solving the equation (4) we get explicit or implicit methods [2]. In order to avoid the iteration inside the optimization iteration the explicit Euler scheme has been used

$$Y^n = Y^{n-1} + \{a(Y^{n-1})Y^{n-1} + f(Y^{n-1})\}h_n \qquad (5)$$

where $h_n = t_n - t_{n-1}$ is the time step. Now instead of the exact equations (3) and (4) we solve discretized equations

$$\widetilde{F}(a(Y^{n-1}), Y^{n-1}, h_n) = Y^n \quad , \quad \text{and} \qquad (6a)$$

$$\widetilde{F}(a(Y^{n-1}), Y^{n-1}, h_n) = Y^{n-1} + \{a(Y^{n-1})Y^{n-1} + f(Y^{n-1})\}h_n \qquad (6b)$$

The non-linear inverse problem (6) has been solved using the *output least squares method* (OLSM). We also have to discretize the distributed unknown parameter $a(y)$ into a certain number of sub-intervals $[y_i, y_{i+1}]$ of arbitrary length $y_{i+1} - y_i$ using suitable almost orthogonal basis functions $a(y) = \sum_{i=1}^{M} N_i(\zeta)\ a_i, \quad \zeta = y/(y_{i+1} - y_i)$. The goal of this method is to find out the least squares solution for vector of the nodal values $\vec{a}_i^{\,*}$ of (9). One seeks unknowns $\vec{a}_i^{\,*}$ such that

$$\left\| \widetilde{F}(\vec{a}_i^{\,*}) - \vec{y} \right\| = \inf_{\vec{a}_i^{\,*} \in D} \left\| \widetilde{F}(\vec{a}_i) - \vec{y} \right\| \qquad (7)$$

where the constraints set D is the class of physically admissible parameters. The data vector $\vec{y}$ is known only within a certain tolerance δ. This approximation $\vec{y}^{\delta}$ satisfying the condition

$$\left\| \vec{y} - \vec{y}^{\delta} \right\| \le \delta \qquad (8)$$

is known (for example due to the scatter in the experimental measurements) and one therefore seeks an $\vec{a}^{\,*}$ minimizing

$$\left\| \widetilde{F}(\vec{a}^{\,*}) - \vec{y}^{\delta} \right\| \qquad (9)$$

Here $\vec{y}_k^{\delta}$ is the vector of measured data. It must be remembered that the number of experimental points y_k^{δ}, called collocation points, should be preferably higher than the number of unknown parameters a_i^* in order to exploit the whole available data. The minimization problem is non-linear. Here either Newton or Conjugate Gradient methods are used.

Because the inverse problem is ill-posed it has to be regularized. In the output least squares method (OLSM) the regularization of the problem is achieved by mesh coarsing and by use of the available a priori known physical constraints on the parameters. An alternative is to do the regularization using *penalized least squares* method [1] that can be regarded as Tikhonov regularization of non-linear problems. In penalized least squares method one seeks a minimum for the functional

$$\left\|\tilde{F}(\vec{a}^*)-\vec{y}^{\delta}\right\|^2+\alpha\left\|L\vec{a}^*\right\|^2 \tag{10}$$

where $\alpha(>0)$ is a regularization parameter depending on the noise level of the data and $L=I$ or some other suitable differential operator depending on the needed regularity of the solution. The first term in equation (10) enforces the consistency of the solution when the second term enforces its stability. An appropriate balance between the need to describe the measurements well and the need to achieve a stable solution is reached by finding an optimal regularization parameter.

APPLICATIONS TO HEAT CONDUCTION PROBLEM

Semi-discretization of the heat conduction equation

Using the standard Galerkin method [3] one obtains the variational form of the heat conduction problem in 1-D as;

$$\int_0^L \rho c\frac{\partial T}{\partial t}v\,dx+\int_0^L \lambda\frac{\partial T}{\partial x}\frac{\partial v}{\partial x}dx=\int_0^L rv\,dx-\left[q_{\omega n}v\right]_0^L \tag{11}$$

with the temperature field approximated by $T^e(x,t)=\mathbf{N}^e(x)\mathbf{T}^e(t)$, where the test and the basis functions are

$$N_1(\xi)=\frac{1-\xi}{2},\quad N_2(\xi)=\frac{1+\xi}{2} \tag{12}$$

The semi-discretization of the heat conduction equation (1) produces the non-linear initial value problem

$$\mathbf{C}(t,\mathbf{T})\dot{\mathbf{T}}(t)=-\mathbf{K}(t,\mathbf{T})\mathbf{T}(t)+\mathbf{f}(t,\mathbf{T}),\quad t>0 \tag{13}$$

$$\mathbf{T}(0)=\overline{\mathbf{T}}_0,\quad t=0 \tag{14}$$

where $\mathbf{T}(t)$ the global vector of degrees of freedom. Equation (13) is an ordinary non-linear differential equation system. Notice that the right hand side corresponds to the force vector $\mathbf{f}(t,\mathbf{T})$, which contains the boundary terms, as also all possible source terms. Equation (16) is to be complemented with appropriate initial conditions (14).

Insulated metal structure

Consider a case of an insulated steel structure. The problem can be dealt as one dimensional problem using two elements (Fig 1). One element is used for the steel part and one element for the insulation part. For the steel part it is assumed that the temperature is uniform (one basis function $N_1 = 1$, one trial function $v = 1$). For the insulation one element with linear interpolation polynomials is used. With these assumptions the global capacity matrix is

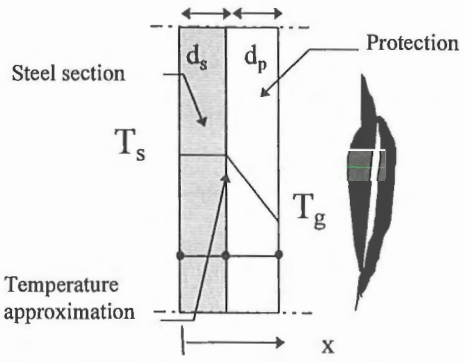

Figure 1. One dimensional idealization of insulated steel structure in fire.

$$\mathbf{C} = \begin{bmatrix} Q_s + Q_{11}^p & Q_{12}^p \\ +Q_{21}^p & +Q_{22}^p \end{bmatrix} \tag{15}$$

where $Q_s = \rho_s A_s c_s(T_s) d_s$ and $Q_{ij}^p = \frac{d_p}{2} \int_{-1}^{1} \rho_p(T(\xi)) c_p(T(\xi)) N_i(\xi) N_j(\xi) A_p \, d\xi$.

The global conductivity matrix is

$$\mathbf{K} = \frac{1}{d_p} \int_{-1}^{1} \lambda_p(T(\xi)) A_p \, d\xi \begin{bmatrix} +1/2 & -1/2 \\ -1/2 & +1/2 \end{bmatrix}. \tag{16}$$

The unknown temperature vector is $\mathbf{T} = \{T_s, T_{pb}\}^T$, where T_s is the temperature of the metal and T_{pb} is the temperature of the fire protection at the boundary x=L=d_s+d_p. We assume an adiabatic boundary condition $q_n = 0$ at x=0 and a prescribed temperature boundary condition $T_{pb} = T_g$ at the boundary x=L. This means that the temperature at the boundary of the insulation is the gas temperature of the surrounding fire. We get only one equation:

$$\dot{T}_s + \frac{\tilde{\lambda}_p A_p / d_p}{Q_s + Q_{11}^p} (T_s - T_g) = -\frac{Q_{12}^p}{Q_s + Q_{11}^p} \dot{T}_g \tag{17}$$

where the notations $\tilde{\lambda} = \frac{1}{2} \int_{-1}^{1} \lambda_p(T(\xi)) d\xi$,

$$Q_s = \rho_s A_s c_s(T_s) d_s \text{ and } Q_{ij}^p = \frac{d_p}{2} \int_{-1}^{1} \rho_p(T(\xi)) c_p(T(\xi)) N_i(\xi) N_j(\xi) A_p \, d\xi \ . \tag{18}$$

have been used.

In the case when thermal conductivities and capacities are constants and do not depend on the temperature the equation (17) will take the form:

$$\dot{T}_s = \frac{\lambda_p A_p / d_p}{c_s \rho_s V_s (1+\phi/3)}(T_g - T_s) - \frac{\phi/6}{1+\phi/3}\dot{T}_g, \tag{19}$$

Here notations $\phi = Q_p / Q_s$, $Q_s = c_s \rho_s V_s$ have been used.

The equation (19) is the same as the equation derived by Melinek and Thomas [4] and considered by them to be the best when $Q_p / Q_s << 1$. The equation is nearly the same as an equation proposed by Wikström [5]:

$$\dot{T}_s = \frac{\lambda_p A_p / d_p}{c_s \rho_s V_s (1+\phi/3)}(T_g - T_s) - [\exp(\phi/10) - 1]\ \dot{T}_g \tag{20}$$

The equation (19) is preferred in applications presented here because no assumption has been made on the gas temperature history. Wikström's solution has been truncated from an analytical solution, where the gas temperature is based on the standard ISO834 curve.

The inverse solution of equation (19) is achieved by minimizing the equation (12), where $y^\delta(t)$ $(\equiv T_s^\delta(t))$ is the measured temperature of the metal structure, $y(t)$ $(\equiv T_s(t))$ is the solved temperature of the metal structure. The discrete coefficient-solution operator (9) is in this case

$$\tilde{F}(T_s^{n-1}, h_n) = T_s^{n-1} + \frac{\lambda_p(T_p^{n-1}) A_p / d_p}{c_s \rho_s V_s (1+\phi/3)}(T_g^{n-1} - T_s^{n-1})h_n - \frac{\phi/6}{1+\phi/3}T_g^{n-1} \tag{21}$$

where $T_p = (T_s + T_g)/2$ is the temperature in the middle of the protection (one Gauss point integration scheme).

Numerical example 1: Steel section protected with intumescent paint

Fire protection materials of steel structures are studied in Nordic countries according to NORDTEST method NT FIRE 021 [6]. In the method the protected steel column is placed in the horizontal furnace. The temperature of the steel and also the gas temperature near the protected section are measured by thermocouples. According to the method NT FIRE 021 the thermal conductivity of the protection material is calculated as a function of time using the equation (26) and the derivatives $\dot{T}_s$ of the measured steel temperature. Small deviations in the measured temperature data may cause large differences in the calculated thermal conductivity. That is why the measured temperature is smoothed.

The method is also applied to intumescent paints that expand during the test and for which the equation is not actually valid. The thermal conductivity is calculated assuming that the material do not expand and maintains its original thickness. The calculated thermal conductivity is then not a real but an effective one that can be used in the design procedure of steel structures.

In the Fig.2b) the thermal conductivities calculated using *ROLSM* are shown. The discrete operator (27) and test results of a commercially available intumescent paint are used. In Figure 2a) the furnace temperature and the measured and calculated temperatures in the steel specimen are shown.

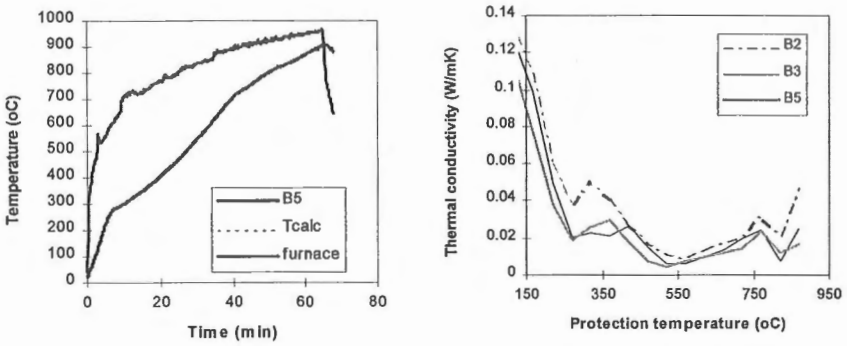

Figure 2a) Furnace temperature, measured and calculated temperature of the steel specimen, b) thermal conductivities of the intumescent paint as a result of the inverse solution. B2, B3 and B5 are the identification numbers of test specimens.

Numerical example 2: Gypsum board.

Cone calorimeter tests in horizontal configuration at a heat flux level of $q_{cone} = 25$ kW/m^2 were performed. The test specimen consisted of a 13 mm thick gypsum board (density 721 kg/m^3) laying on a 30 mm thick layer of mineral wool (Fig. 2). The surface area exposed to the heat flux was A_1=100 mm x 100 mm. There was a 10 mm thick aluminium plate under the gypsum board in the second test. In the first test, there was no aluminium plate present.. The temperature of the upper surface of the gypsum board was measured using an infra-red temperature measuring device The temperature profile inside the specimen as a function of time was measured.

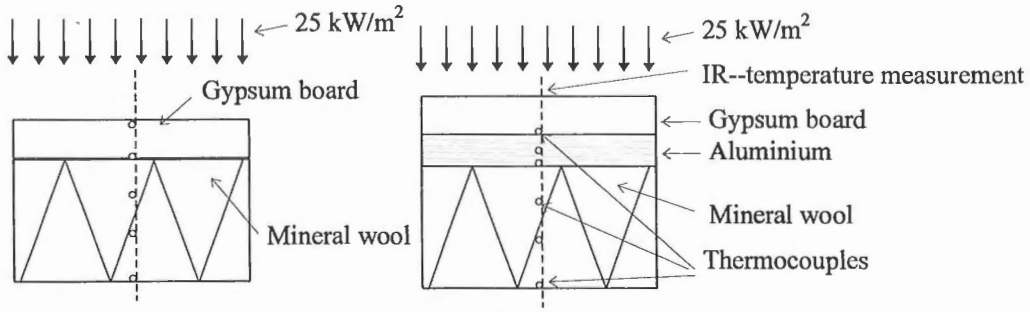

Figure 3. Idealized test arrangements in cone calorimeter tests. a) test without aluminium plate b) test with aluminium plate.

In the first test case (without aluminium plate) the specific heat of the gypsum board was calculated. The specific heat is discretized using piece-wise linear basis functions with respect to the temperature $c(T) = \sum N_j a_j(T)$. The conservation of energy in the gypsum board can be written as

$$\int_V \rho c \dot{T} dV = -\int_{\partial V} \vec{q} \cdot \vec{n} d\Gamma + \int_V \rho r dV \qquad (22)$$

The source term in the equation is incorporated into the effective specific heat. The equation (22) reads as

$$\dot{\tilde{T}}(t) = +q_{cone} \frac{A_1}{\rho c(\tilde{T}) V} \equiv f(T(x;t),t) \qquad (23)$$

where the function $\tilde{f}$ is defined by $\tilde{f}(t) = 1/d \int_d f(x;t)dx$. The ODE (29) is integrated numerically using an implicit Euler scheme;

$$\tilde{T}(t_{k+1}) = \tilde{T}(t_k) + \int_{t_k}^{t_{k+1}} f(\tilde{T}(\tau),\tau)d\tau \approx \tilde{T}(t_k) + f(\tilde{T}(t_k),t_k)h_k \qquad (24)$$

The specific heat capacity *c(T)* was the regularized solution of the constrainted minimization problem

$$\min\left(\left\| \tilde{T}(t) - \tilde{T}_{calc.}(\vec{a};t) \right\|^2 + \alpha \left\| L\vec{a} \right\|^2 \right), \quad with\ a_j \in D(\vec{a}) \qquad (25)$$

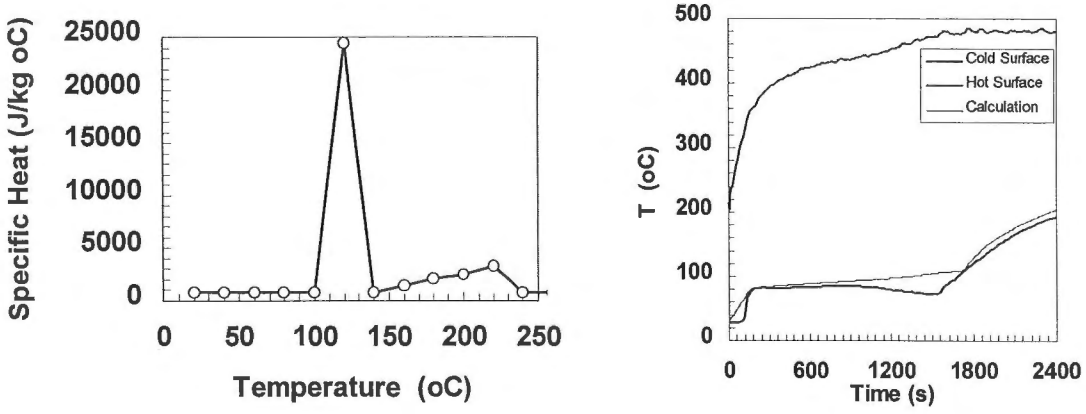

Figure 4!. a) Calculated specific heat of the gypsum board measured in a cone calorimeter experiment at 25 kW/m^2. b) Measured surface temperature, bold lines, the calculated in thin line.

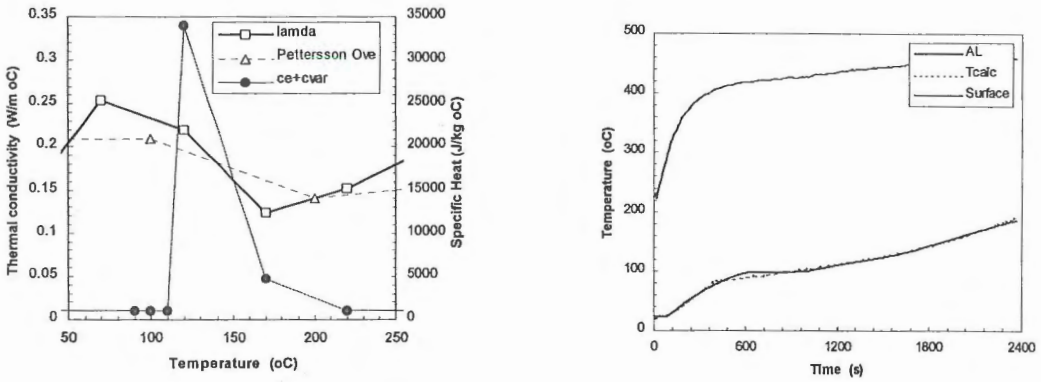

Figure 5. a) Calculated specific heat and thermal conductivity of the gypsum board measured in a cone calorimeter experiment at 25 kW/m^2. Test data for the thermal conductivity according to Pettersson [7] is shown for comparison. b) Measured surface temperatures and the temperature of the aluminium plate, bold lines, the calculated in dotted thin line.

The solution is seeked from the domain of physically addmissible functions which takes into account the possible range of the unknown parameters a_j The equation (31) is nonlinear. The solution is found using Newton method with the discrepancy principle as the stopping criteria. This means that the Newton iteration number n during the iterative solution of minimization (25) is stopped when the residual $\left\| \tilde{T}^{\delta}(t) - \tilde{T}_{calc.}(\vec{a}^{\delta}_{\alpha(n)};t) \right\| \approx R\delta$ is reached for the first time, with R = 1.6 and α = 0.00001. The accurancy of the temperature measurements is assumed to be $\left\| \tilde{T}^{\delta}(t) - \tilde{T}(t) \right\| \leq \delta \approx \int_{t_\infty} 2^{o} Cdt \approx 98^{o} Cs$.

The results of the calculations are shown in Fig. 4. The relative amount of humidity (mass of water / total mass of gypsum) in the gypsum board was calculated from the peak of the specific heat and was found to be equal to 21 %. Experimental results show that the the water content of gypsum boards is about 18 % in the temperature range < 200 °C.

The second test specimen was similar to the first one execpt directly under the gypsum board 10 mm thick aluminium plate was present. The temperature of the test specimen was recorded as in the first example. The temperature distribution inside the gypsum board was approximated to be linear and the aluminium temperature a constant. Equation (25) with discretization (27) was used in modelling the direct problem. Here both the specific heat and the thermal conductivity were discretized using piece-wise linear basis functions with respect to the temperature. Figure 5 shows the results. The thermal conductivity of gypsum according to Pettersson [7] is shown for comparison.

Bare metal structure and numerical example: aluminium specimen in heated oven

Consider a bare metal structure without fire protection (Fig. 6). We use only one finite element with one basis function $N_1 = 1$ which is the same as assuming the temperature to be constant in the solution domain. Applying the Galerkin method ($\nu = 1$) the variational formulation is following:

$$\int_0^{d_s} c_s(T)\ \rho_s(T) A_s dx\ \dot{T} = q_n(0)\ A_{\Gamma 0} - q_n(L)\ A_{\Gamma L} \tag{26}$$

Assume the radiative and convective boundary conditions at the boundary x=L.; $q_n(L) = h_c(T_s - T_g) + \varepsilon\ \Phi\sigma\ (T_s^4 - T_g^4)$. The structure and gas are assumed to be two infinitely long parallel plates, for which the following relation applies: $\varepsilon\ \Phi_{1-2} = \varepsilon_r = (1/\varepsilon + 1/\varepsilon_g - 1)^{-1}$. Here ε is the emissivity of the structure and ε_g is the emissivity of the gas and ε_r is the resultant emissivity. We also combine the two boundary conditions in a following way: $\tilde{h}(T, T_c) = h_c + \varepsilon_r\, \sigma(T^2 + T_c^2)(T + T_c)$ and get finally an equation:

$$\dot{T}_s = \frac{\tilde{h}\ A_{\Gamma L}(T_g - T_s)}{c_s(T)\ \rho_s(T) A_s\ d_s} + \frac{q_n(0)\ A_{\Gamma 0}}{c_s(T)\ \rho_s(T) A_s\ d_s} \tag{27}$$

We may now assume that the heat flow through the boundary is a function of the temperature of the metal structure $q_n = q_n(0, T_s)$. If the heat flow through the boundary is not taken into account (q_n=0) the equation (27) will take the traditional form used in the fire design of steel structures.

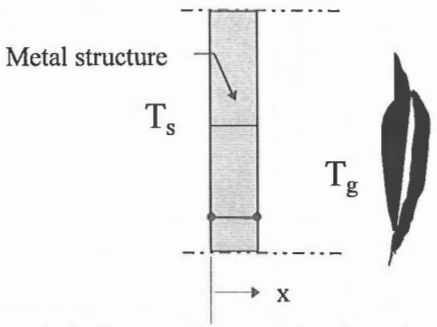

Figure 6. One dimensional idealization of an uninsulated metal structure in fire.

Consider a case were an uninsulated aluminium specimen is placed in an oven in order to be tested at high temperatures. The specimen is surrounded by the oven, but the ends of the specimen are clamped into the steel rods, so a part of the heat flow escapes through the ends of the specimen. The problem is dealt as one dimensional according to equation (29), where the heat loss $q_n = q_n(0, T_s)$ has been assumed to be function of the aluminium temperature. The inverse solution of the equation (29) is achieved by minimizing equation (12), where

$y^{\delta}(t)\ \left(\equiv T_s^{\delta}(t)\right)$ is the measured and $y\ (t)\ \left(\equiv T_s\ (t)\right)$ the solved temperature of the aluminium structure. In this case the discrete coefficient-solution operator is:

$$\widetilde{F}(T_s^{n-1},h_n)=T_s^{n-1}+\frac{\widetilde{h}(T_g^{n-1},T_s^{n-1})\ \ A_{\Gamma L}(T_g^{n-1}-T_s^{n-1})}{c_s\ \rho_s A_s\ d_s}h_n+\frac{q_n(T_s^{n-1},0)\ \ A_{\Gamma 0}}{c_s\ \rho_s A_s\ d_s}h_n \qquad (28)$$

where $A_{\Gamma L}$ is the area of the specimen exposed to the heat and $A_{\Gamma 0}$ is the sum of the areas of the ends ef the specimen.

The tests have been carried out at HUT in the Laboratory of Structural Mechanics using the test facilities of the Laboratory of Steel Structures in a project dealing with the high temperature properties of aluminium. The temperature of the oven was controlled to obtain a constant temperature of the specimen during the steady-state tests. In transient tests the oven temperature had a fixed changing rate, which was hoped to cause constant temperature rate of the specimen. The heat flow through the ends of the specimen and the slow heating rate at the beginning were problematic. The reason for the problems was the good conductivity and low emissivity of the aluminium.

Parameters $\varepsilon, q_n(T_s,0)$ were approximated as piecewise linear functions of the aluminium specimen temperature T_s. Convection coefficient h was assumed to be constant. The parameters were solved by fitting a one test. The solved parameters are shown in Fig 6a. The measured temperatures of the oven and specimen and also the calculated temperature of the aluminium specimens are shown in the Figures 7b and 8a-b.

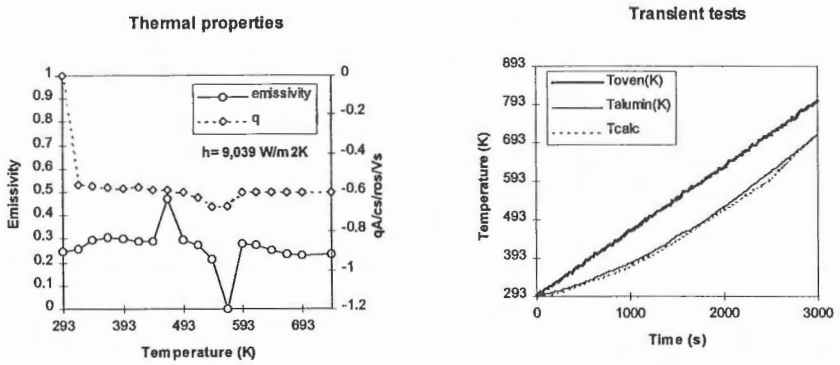

Figure 7a) Thermal properties obtained by the inverse solution b) measured and calculated temperatures of aluminium specimen in heated oven, transient test.

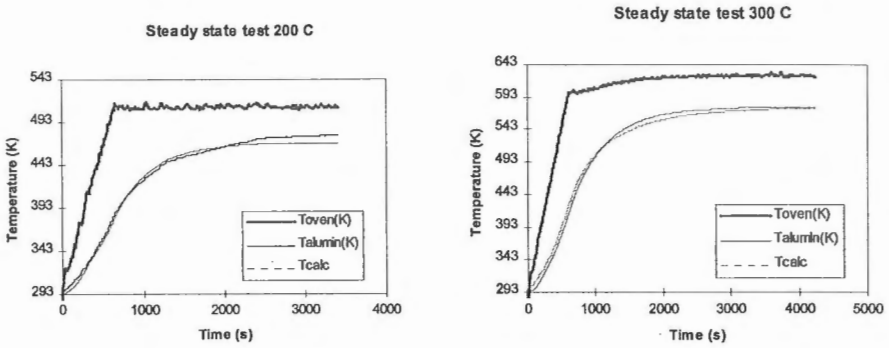

Figure 8a) and b) Measured and calculated temperatures of aluminium specimen in heated oven.

IDENTIFICATION OF MULTIPLICATIVE VISCOPLASTICITY LAW

The uniaxial expression of the multiplicative model presented by Chaboche and Lemaitre [8] including the linear elasticity law, viscosity -hardening law is

$$\varepsilon = \varepsilon_e + \varepsilon_p + \varepsilon_T$$
$$\sigma = E(T)\varepsilon_e \tag{29}$$
$$\sigma = K(T)\varepsilon_p^{1/M(T)}\dot{\varepsilon}_p^{1/N(T)}$$

where N, M, K and E are three material parameters, which are functions of the temperature T. N is the viscosity exponent, M is the hardening exponent, K is the coefficient of resistance and E is the modulus of elasticity, ε_e is the linear elastic, ε_p the viscoplastic, ε_T the thermal strain and $\dot{\varepsilon}_p$ is the rate of the viscoplastic strain. The viscosity exponent N has a value of the order of 2 for very viscous materials and of 100 for slightly viscous materials which warrant a plasticity law; the hardening exponent M varies approximately between 2 and 70; the magnitude of the coefficient of resistance K varies from 100 to 10 000 MPa. The different results from tension tests, creep tests and relaxation tests can be predicted with a constitutive law with three parameters which represent the viscoplastic phenomena under monotonically increasing strain ($\dot{\varepsilon} \geq 0$) rather well.

The hypothesis of partitioning the total strain into an elastic and inelastic, viscoplastic strains has been used in the law. An instantaneous plastic strain has been assumed to be nonexistent in the framework of the present treatment.

We may interpret equation (30) in terms of a coefficient-to-solution operator $F(\vec{a}(T),\varepsilon_\sigma,t)=\varepsilon_\sigma$, where

$$F(\vec{a}(T),\varepsilon_\sigma,t)=\int_0^t\left(\frac{\sigma}{E(T)}\right)^{N(T)}\left(\varepsilon_\sigma-\frac{\sigma}{E(T)}\right)^{-N(T)/M(T)}dt+\frac{\sigma}{E(T)} \tag{30}$$

and $\vec{a}(T)=(K(T),M(T),N(T),E(T))^T$ is the vector of unknown parameters and $\varepsilon_\sigma=\varepsilon-\varepsilon_T$ is the stress dependent part of the total strain.

When explicit Euler scheme is used one gets instead of exact operator an approximation; $\tilde{F}(\vec{a}(T),\varepsilon_\sigma,t)=\varepsilon_\sigma^n$, where

$$\tilde{F}(\vec{a}(T),\varepsilon_\sigma^{n-1},t)=\varepsilon_\sigma^{n-1}+\left(\frac{\sigma^{n-1}}{E(T)}\right)^{N(T)}\left(\varepsilon_\sigma^{n-1}-\frac{\sigma^{n-1}}{E(T)}\right)^{-N(T)/M(T)}h_n+\frac{\sigma^{n-1}}{E(T)} \tag{31}$$

The whole temperature interval studied is discretized into a chosen number of subintervals $[T_i,T_{i+1}]$. The parameters a (= $K(T),M(T),N(T),E(T)$) are approximated as piecewise linear functions of temperature: $a(T)=(1-\xi)a_i+\xi\ a_{i+1}$ for each temperature interval $T\in[T_i,T_{i+1}]$, $\xi=T/(T_{i+1},T_i)$, separately. Higher polynomial approximations were avoided, because they cause problems in the stability of the solution if the polynomial functions do not form an orthogonal base. The unknown parameters were seeked to minimize:

$$\left\|\tilde{F}(\vec{a}(T),\varepsilon_\sigma^{n-1},t)-\varepsilon_k^\delta\right\| \tag{32}$$

Both steady-state and transient tests were conducted for aluminium alloy AA6063-T6 at high temperatures at HUT, Laboratory of Structural Mechanics. The test results have been used in the identification of the law. The hardening tests at constant temperature (steady-state tests) were carried out with two equal tests at deformation rate 0,18 mm/min and one test at deformation rate 1,8 mm/min at temperatures 100 °C, 150 °C, 200 °C, 225 °C, 250 °C and 300 °C. Three tensile tests were carried out at room temperature to determine the mechanical properties of aluminium alloy AA 6063-T6 at room temperature.

In the transient creep tests (constant load, varying temperature) the oven was controlled so that the oven gas temperature rate was 10 K/min. Transient state tensile tests were carried out with two equal tests at each stress level of 3, 20, 40, 60, 80, 100, 120, 140, 160, 180 and 190 MPa. The thermal strain of the aluminium alloy was determined with three tests at load level 3 MPa. At first, the parameters were solved at constant temperatures $T_i=100$ °C, 150 °C, 200 °C, 225 °C, 250 °C and 300 °C using the steady-state results at two deformation rates. After that some of the transient results were used to calculate parameter values at temperature range 20 °C-400 °C using the temperature step 25 °C.

Figures 9a show the values of Young's modulus E and coefficient of resistance K as a function of temperature. In Fig. 9b the viscosity and hardening exponents N, M obtained by the minimi-

zation algorithm are shown. In Figures 10-11 both the experimental results and calculated ones are illustrated. It can be seen that the multiplicative viscoplasticity law of Chaboche and Lemaitre satisfactorily predicts behaviour of aluminium alloy AA6063-T6 in transient tests and in steady state tests of different strain rates.

CONCLUSIONS AND ACKNOWLEDGEMENTS

Several applications of the regularized output least square method (ROLSM) to the parameter identification of the heat transfer in insulated and bare metal structures were presented. For each problem one ordinary differential equation was derived from the variational formulation of the general heat conduction problem. Although, the examples shown consist only of a one ODE, the method is directly applicable to the system of ODE obtained by the semi-discretization of the variational formulation. As an example of the use of the method to determine mechanical properties of metals, an identification of multiplicative viscoplasticity law for aluminium alloy AA6063-T6 was illustrated. In the case of a constitutive equation identification, the method can be generalized to tests where several components of the strain rate tensor are considered as well.

The authors hope that the small variety of problems presented in this paper reveal the huge possibities that the use of systematic methods of variational formulation (FEM) and the inverse solution technique (ROLSM) has to offer to modelling and to model identification.

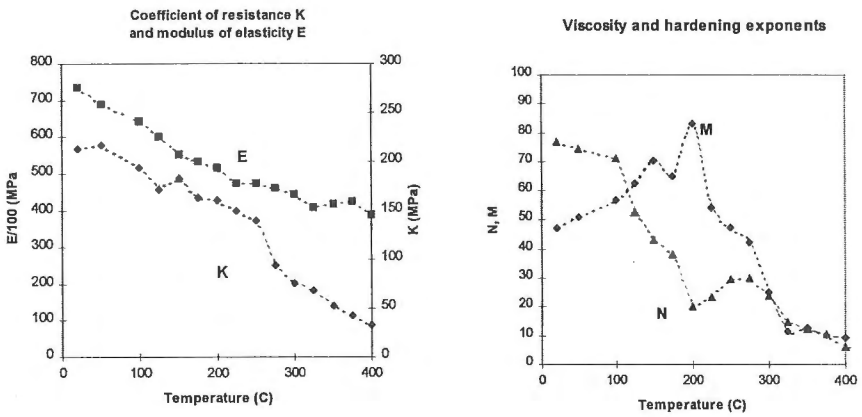

Figure 9. The parameters of the multiplicative viscosity law for aluminium alloy AA6063-T6 as a result of the ROLSM inverse solution.

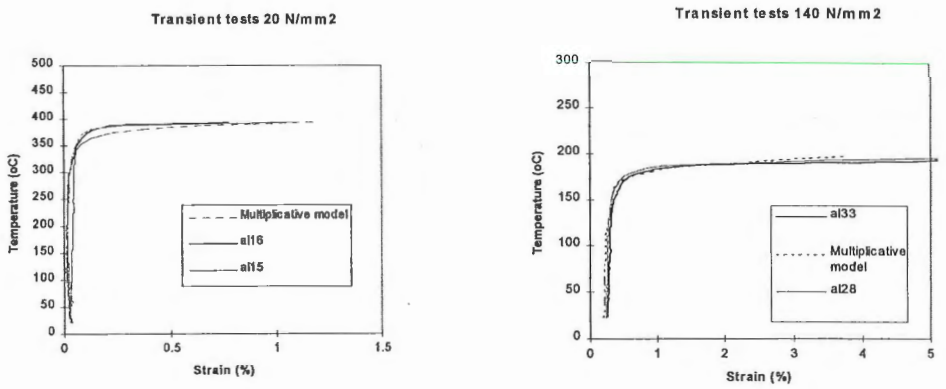

Figure 10a) Transient test results(al15,al16, al28, al33) and calculated solution (dotted line) at stress level 20 N/mm^2 and b) 40 N/mm^2.

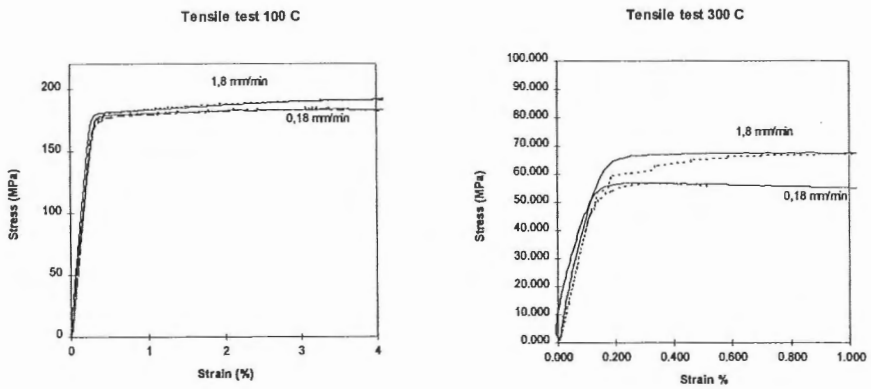

Figure 11 a) Hardening test results and calculated solution at temperature 100 °C and at temperature 300 °C

The applications presented in this paper were developed in "VTT/STEEL" program funded by VTT Building Technology. and in the research program " Properties of aluminium at high temperatures" going on at HUT at the Laboratory of Structural Mechanics funded by the Technology Development Centre of Finland (TEKES). The authors wish to thank the members of the advisory committee of the aluminium program for giving a permission to publish the aluminium project results. Mr. Outinen, who has carefully carried out the long test series of the aluminium program deserves special thanks.

REFERENCES

[1] C.W. Groetsch, Inverse Problems in the Mathematical Sciences, *Wieweg Mathematics for Scientists and Engineers, Vieweg, 1993* pp.151.
[2] J. Pitkäranta, Difference methods, *Lecture notes, Helsinki University of Technology.*
[3] B. Szabo, I. Babuška. Finite Element Analysis, *John Wiley & Sons, 1991*, pp. 357.
[4] S.J.Melinek, P.H. Thomas. Heat Flow to Insulated Steel, *Fire Safety Journal, 12 (1987)* pp.1-8
[5] U. Wickström, Temperature Analysis of Heavily-insulated Steel Structures Exposed to Fire, *Fire Safety Journal, 9 (1985)* 281-285.
[6] Nordtest method NT FIRE 021, NORDTEST 1985.
[7] O. Pettersson, K. Ödeen, Brandteknisk dimensionering, *Liberförlag, Stockholm 1978*, pp.181
[8] J. Lemaitre, J.-L. Chaboche, *Mechanics of solids*, Cambridge University Press 1994, pp.556.

Jukka Myllymäki, MSc Tech
Researcher at VTT Building Technology, Fire Technology
Visiting Researcher at HUT Laboratory of Structural Mechanics

Djebar Baroudi, MSc Tech
Researcher at VTT Building Technology, Fire Technology